HIGH-VELOCITY IMPACT DAMAGE BEHAVIOR OF GRAPHITE-EPOXY COMPOSITE LAMINATES

K. Woo[1*], I. Kim[2], S.C. Ha[2], H. Shin[2], and J.H. Kim[3]
[1] School of Civil Engineering, Chungbuk National University, Cheongju, Korea
[2] Department of Aerospace Engineering, Chungnam National University, Daejeon, Korea
[3] Agency for Defense Development, Daejeon, Korea
[*]Corresponding author(kw3235@chungbuk.ac.kr)

Keywords: *high-velocity impact, composite laminates, impact damage, acoustic emission, failure analysis, penetration velocity, element erosion*

1 Introduction

The high-velocity impact of small objects can cause severe damage to the laminated composite structures (e.g., Refs. [1-3]). Proper understanding of high-velocity impact damage behavior is one of the key elements for the establishment of structural integrity for aerospace structures, and thus, has been the focus of many researches over the past several decades (e.g, Refs. [4-5]).

In this study, a series of high-velocity impact tests were performed to investigate the impact damage behavior of laminated composites. In the experiment, the air gun impact tester was used, and the ballistic and residual velocity was measured. Also, the acoustic emission of the laminate was recorded for further examination. In the analysis, a numerical simulation procedure was developed in which LS-DYNA finite element models were generated and analyzed. The simulation results were compared to those of the experiments. Continuum damage theory was applied in FE simulation to predict the damage mode and extent. The analysis results were systematically investigated, focusing on predicting accurately the penetration velocity of the projectiles, as well as the damage behavior of the laminated composites.

2 Experiment

The experimental set-up and specimen are shown in Fig. 1. The specially fabricated compressed air gun impact tester was used to fire a 6.5 mm diameter (1.1 gram) steel ball at various impact velocities on to the composite panel. The facility consists of a pressurized air tank, gun barrel, four high precision magnetic velocity sensors for measuring the steel ball velocity, AE (acoustic emission) sensor and supporting fixtures. The velocity limit of the air gun is approximately 325 m/s. The two magnetic sensors are mounted at the end of gun barrel at a distance of 10 cm apart and the other two magnetic sensors are mounted at the rear of impact specimen for measuring the residual velocity after penetration.

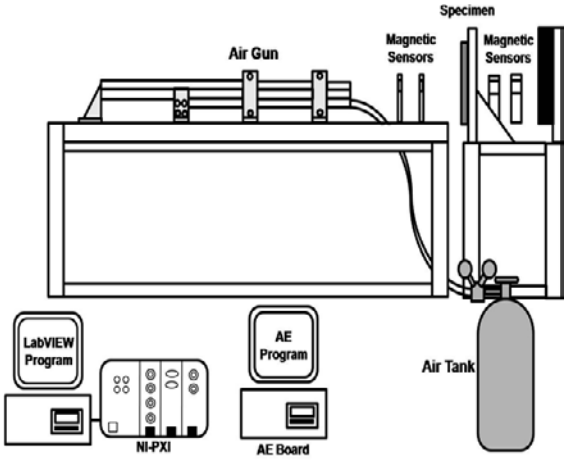

(a) Air-gun impact tester

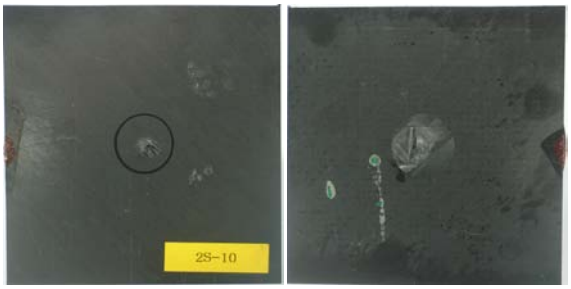

(b) Impact specimen

Fig. 1. Experimental set-up.

The AE sensors of UT-1000 (Physical Acoustics, Inc.) were attached on the specimen to record the signal during the impact. The property of the AE sensor was summarized in Table 1 [6].

Table 1. AE sensor property.

AE sensor	Type	Peak freq. (kHz)	Operation freq. range (kHz)
UT-1000	Wide	503.91	100 – 950

Table 2 shows the dimensions of composite specimen. The specimens used in this study were laminates made of graphite/epoxy unidirectional prepreg (USN 150B) with $[45/0/-45/90]_{nS}$ stacking sequence. The specimen was placed on a rigid support with a circular hole and clamped by a steel fixture without preload. The portion of the specimen located at the hole (the circled region in Fig. 1(b)) was the deformable portion. In this study, 2 cases of different stacking sequences with 16 and 24 plies were considered.

Table 2. Specimen dimensions (*d*: diameter of deformable circular region of laminates).

No. of plies	Stacking sequence	*d* (mm)	Thickness (mm)
16	$[45/0/-45/90]_{2S}$	25.4	2.256
24	$[45/0/-45/90]_{3S}$	25.4	3.384

To validate the approach and damage model of high velocity impact, a series of experimental impact tests based on the air gun impact tester were performed at distinct energy levels for various specimens. For the validity of the data, four tests were conducted for each case. The sensor signals were recorded at a rate of 1MHz by DAQ system (PXI, NI) for the further analysis.

Table 3 summarizes the experimental results. The test was performed with various impact velocities (v_i). The penetration occurred at v_i = 167 m/s for the 16 ply laminate, and v_i = 223 m/s for the 24 ply laminate. Below these impact velocities, penetration was not occurred. One can also see that the residual velocity increased as the initial impact velocity increased.

Fig. 2 shows the photos of impacted specimen when d/D = 4 and the number of plies = 24. The initial impact velocity was 223 m/s. At this velocity the impactor penetrated the laminate with the residual velocity of 34.83 m/s. As can be seen in the figure, an extensive amount of damage occurred at the back surface of the laminated specimen. The damage propagation was constrained by the rigid boundary.

Table 3. Impact test results.

No. of plies	Stacking sequence	Impact velocity (m/s)	Residual velocity (m/s)
16	$[45/0/-45/90]_{2S}$	155	–
		167	26.8
		184	86.4
24	$[45/0/-45/90]_{3S}$	211	–
		223	34.8
		240	48.5

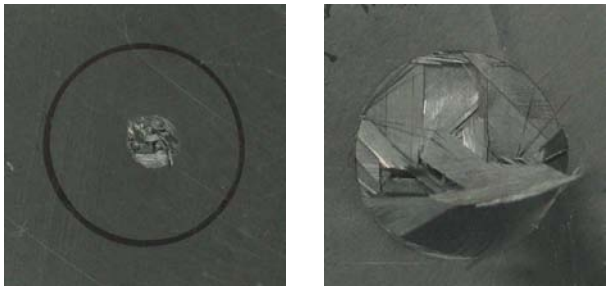

(a) Front surface (b) Back surface

Fig. 2. Photos of front and back surfaces of damaged specimen (d/D = 4 and the number of plies = 24, v_i = 223 m/s).

3 Numerical Analysis

In this study, the commercial explicit nonlinear finite element code LS-DYNA was used to simulate the high-velocity impact event to predict the impact damage of composite laminates. The composite laminates were modeled by shell elements, and ENHANCED_COMPOSITE_DAMAGE MAT54 model was used. The failure criterion of this material model is give as follows.

Tensile fiber mode:

$$e_f^2 = \left(\frac{\sigma_{aa}}{X_t}\right)^2 + \beta\left(\frac{\sigma_{ab}}{S_c}\right)^2 - 1 \quad (1)$$

Compressive fiber mode:

$$e_{fc}^2 = \left(\frac{\sigma_{aa}}{X_c}\right)^2 - 1 \quad (2)$$

Matrix tensile mode:

$$e_m^2 = \left(\frac{\sigma_{bb}}{Y_t}\right)^2 + \left(\frac{\sigma_{ab}}{S_c}\right)^2 - 1 \quad (3)$$

Matrix compressive mode:

$$e_d^2 = \left(\frac{\sigma_{bb}}{2S_c}\right)^2 + \left[\left(\frac{Y_c}{2S_c}\right)^2 - 1\right]\frac{\sigma_{bb}}{Y_c} + \left(\frac{\sigma_{ab}}{S_c}\right)^2 - 1 \quad (4)$$

In equations (1) – (4), failure was considered to occur when the values were greater than zero. Only the deformable portion of the laminates was included in the FE model and the clamped boundary conditions were applied at all sides. Theoretically the impact damage would occur cyclic-symmetrically for the considered configuration. The cyclic-symmetry can be modeled through an MPC type condition. In this study, however, the whole portion of the composite laminates was modeled instead. The impact projectile was also modeled by thin shell elements with MAT20 rigid material model. The density was adjusted to give the same projectile mass.

The interaction between the impact projectile and the composite panel was considered using ERODING_SURFACE_TO_SURFACE contact option. Laminate elements were deleted when the erosion criterion was satisfied.

Table 4 shows the lamina properties used in this study. The analysis parameters were fine-tuned first by comparing the results for selected test cases [4]. Then these were used to predict the penetration impact velocities and the extent of impact damage.

Table 4. Material properties of USN 150B graphite/epoxy lamina

Density (ton/mm^3)	ρ	
Thickness (mm)	t	0.141
Fiber modulus (GPa)	E_{11}	131
Transverse modulus (GPa)	$E_{22} = E_{33}$	8.2
Shear modulus in 12/13 dir. (GPa)	$G_{12} = G_{13}$	4.5
Shear modulus in 23 dir. (GPa)	G_{23}	3.5
Poisson's ratios	$\nu_{12} = \nu_{13}$	0.28
	ν_{23}	0.47
Fiber tensile strength (MPa)	X_T	2,000
Fiber compressive strength (MPa)	X_C	2,000
Transverse tensile strength (MPa)	$Y_T = Z_T$	61
Transverse comp. strength (MPa)	$Y_C = Z_C$	200
Shear strength	S	70

Table 5 summarized the analysis results. The predicted residual velocities match reasonably well to the test results in Table 3.

Fig. 3 shows the variation of impactor velocity versus time. As can be seen in the figure, the impactor velocities decreased rapidly due to the initial contact. Then a short duration followed with constant speed in which the laminate moved away from the impactor. Then the velocity decreased again as the second contact occurred. The impactor velocities continuously decreased and changed sign indicating bouncing back without penetration when the initial velocity was 155 m/s for 16 ply case, and 211 m/s for 24 ply case. For the other cases, the velocities reached lower peak points, increased slightly due to the inverse contact, and then became constant penetrating completely through the laminates.

Table 5. Predicted residual velocity.

No. of plies	Stacking sequence	Impact velocity (m/s)	Residual velocity (m/s)
16	$[45/0/-45/90]_{2S}$	155	-23.39
		167	35.25
		184	65.65
24	$[45/0/-45/90]_{3S}$	211	-30.29
		223	45.22
		240	57.20

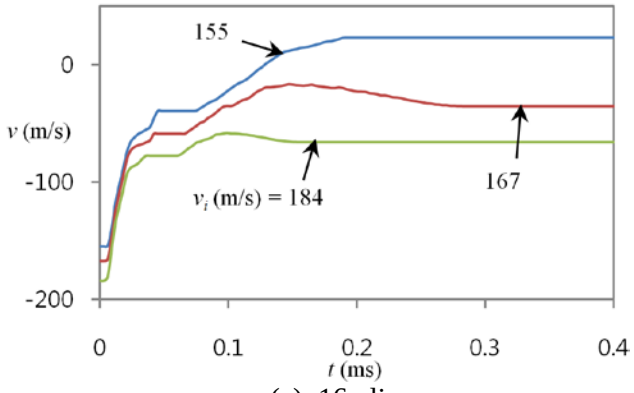

(a) 16 plies

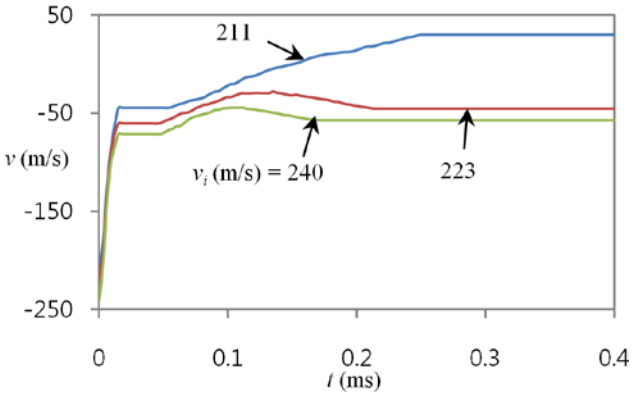

(b) 24 plies

Fig. 3. Time history of impactor velocity.

The time history of contact forces are shown in Figs. 4-5. All cases showed very high contact forces for the initial contacts, while the forces of the second contacts were significantly smaller. This indicates major portion of the impact damage occurred during the first contact. One can see that while the contact forces were always positive for the cases where the penetration was not occurred (Fig. 4(a) and Fig. 5(a)), small negative contact forces occurred at the later stage for the cases where the penetration occurred. This was the inverse contact and had the effect of pushing forward the impact projectile, and thus increasing the residual velocity. One can also observe that the contact duration time decreased as the difference between the impact velocity and the penetration impact velocity increased.

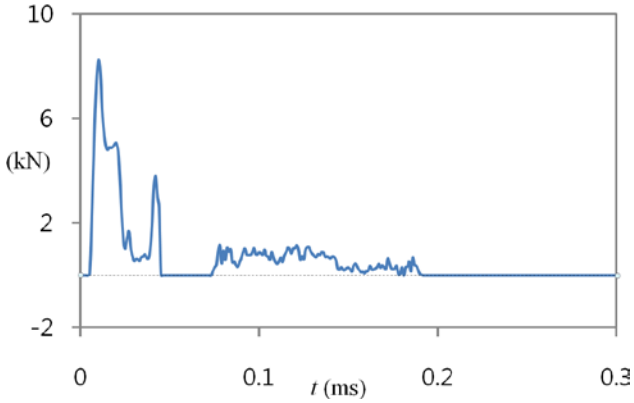

(a) v_i = 155 m/s

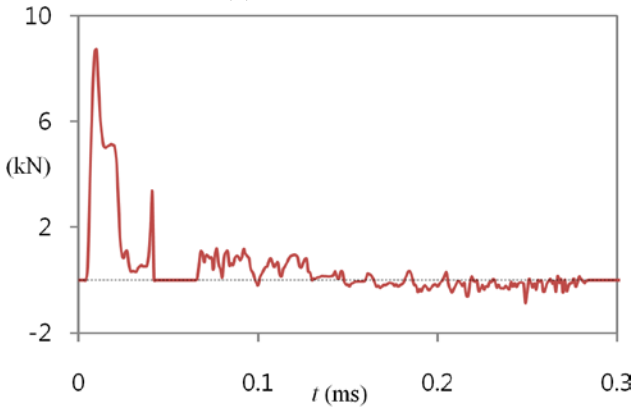

(b) v_i = 167 m/s

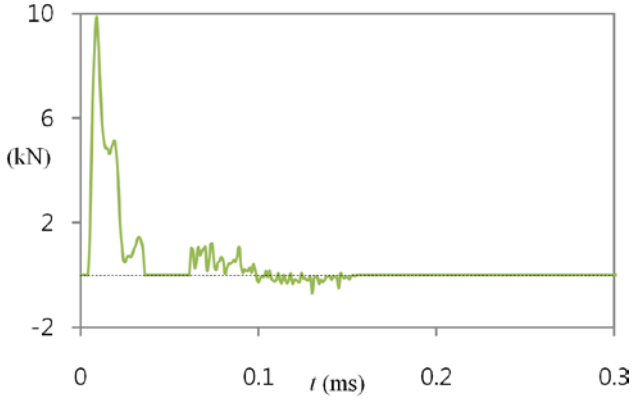

(c) v_i = 184 m/s

Fig. 4. Time history of contact forces for 16 ply laminates.

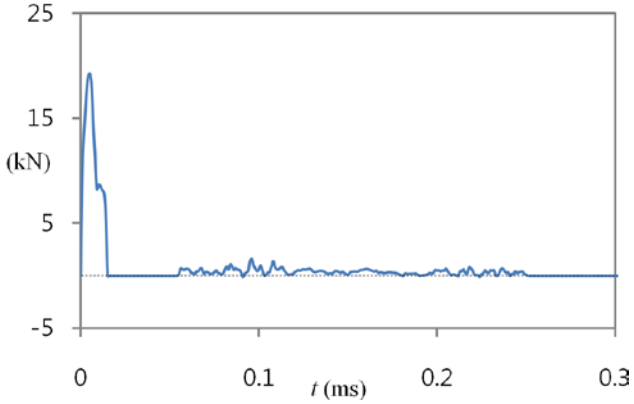

(a) v_i = 211 m/s

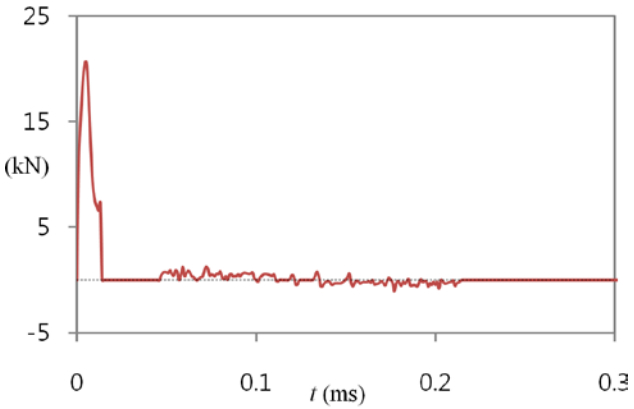

(b) v_i = 223 m/s

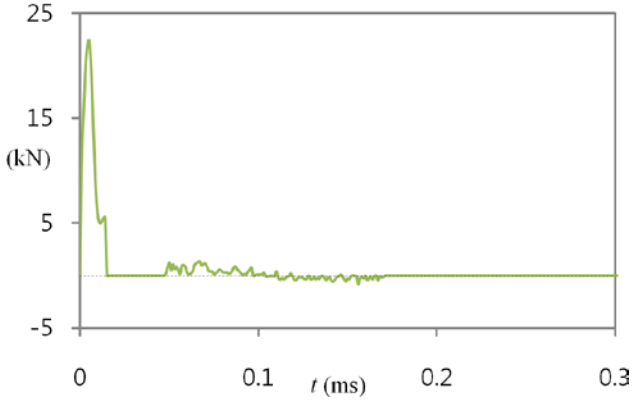

(c) v_i = 240 m/s

Fig. 5. Time history of contact forces for 24 ply laminates.

Figs. 6-7 show the fiber tension damage (f_1) for the back surface plies and the fiber compression damage (f_2) for the front surface plies, respectively, at t = 9 μs for the 24 ply case with v_i = 223 m/s. Here, '1' indicates the material was undamaged and '0' indicates the fiber damage occurred completely. As expected, initially the fiber tensile damage (f_1) occurred in the laminas located at the back surface, while the fiber compressive failure dominated the damage in the laminas located at the front surface. Also, the damage occurred in the orthogonal direction to the fiber direction.

Conclusion

In this study, tests and analysis were performed to investigate the high velocity impact damage behavior of laminated composites. In the experiment, a 6.35-mm steel ball was impacted on the circular shape $[45/0/-45/90]_{nS}$ quasi-symmetrically stacked laminates with 16 and 24 plies. The ballistic and residual velocity was measured for various initial impact velocities. In the analysis, finite element simulations were performed using LS-DYNA. Results indicated that the predicted residual velocities were matched well with those by experiment. From the analysis results, the velocity history was examined and the effect of the impact force history was discussed. The detailed time history of damage modes and shapes was also predicted.

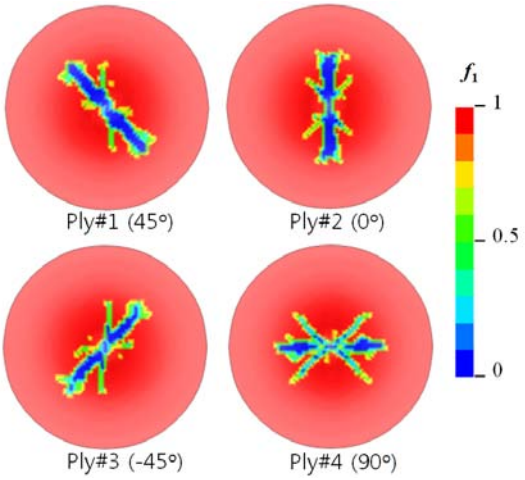

Fig. 6. Fiber tensile failure indexes of back surface layers at t = 9 μs.

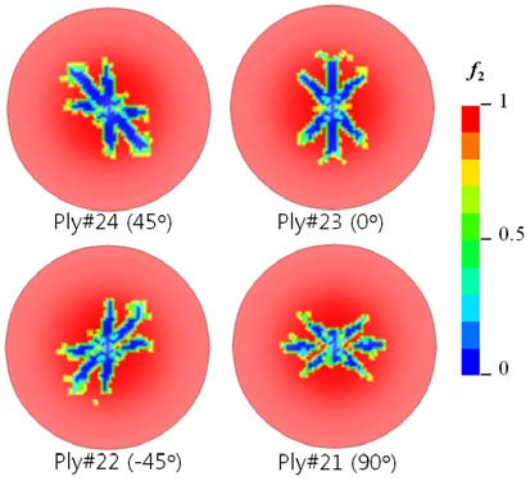

Fig. 7. Fiber compressive failure indexes of back surface layers at t = 9 μs.

Acknowledgement

This work was supported by the Agency for Defense Development (ADD-10-01-08-17).

References

[1] Y. Tanabe, M. Aoki, "Stress and strain measurements in carbon-related materials impacted by a high-velocity steel sphere", *Int. J. Impact Engineering*, 2003, Vol.28, pp. 1045-1059.

[2] A.C. Okafor, A.W. Otieno, A. Dutta, and V.S. Rao, "Detection and characterization of high-velocity impact damage in advanced composite plates using multi-sensing techniques", *Composite Structures*, 2001, Vol.54, pp. 289-297.

[3] J.H. Shih and A.K. Mal, "Acoustic Emission from Impact Damage in Cross-ply Composites," Proceedings of *Structural Health Monitoring*, 2000, pp. 209-217.

[4] K. Schweizerhof, W. Weimar, T.M. Munz, and T. Rottner, "Crashworthiness Analysis with Enhanced Composite Material Models in LS-DYNA – Merits and Limits", 5th International LS-DYNA Conference, 1998.

[5] M. Loikkanen, G. Praveen, and D. Powell, "Simulation of Ballistic Impact on Composite Panels", 10th International LS-DYNA Users Conference, 2008.

[6] W.H. Prosser, M.R. Gorman and D.H. Humes, "Acoustic Emission Signals in Thin Plates Produced by Impact Damage", Journal of Acoustic Emission Vol. 17(1-2), (June, 1999), pp. 29-36.